Center for Earth Observation and Digital Earth
Chinese Academy of Sciences

Urban Impervious Surfaces Extraction from RADARSAT-2 PolSAR Data Using SVM Method

Xinwu LI, Huadong Guo, Zhongchang Sun

Center for Earth Observation and Digital Earth(CEODE),
Chinese Academy of Sciences(CAS)

Dragon 2 Symposium 20- 24 June 2011 Prague, Czech Republi

Outline

- Introduction
- Study area and datasets
- Methods
- Results and analysis
- Conclusions

Introduction

Land Change in Tai Lake region, China from 1973 to 2005

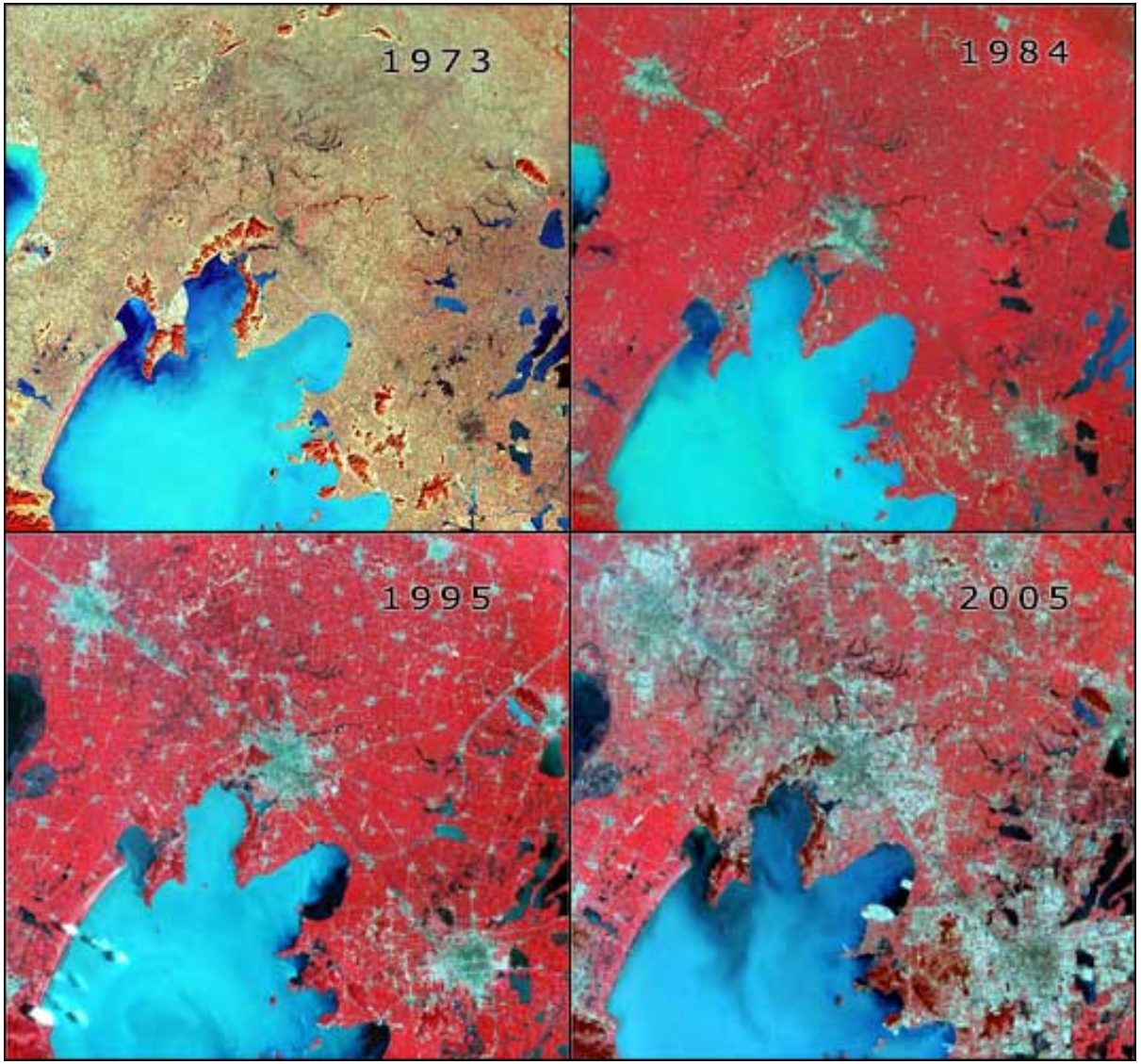

Introduction

- Land use/land cover (LULC) changes have been treated as one of the most important sensitive factors for global environmental change.
- Urbanization is the major force that is driving LULC changes.
- Although urbanization due to urban sprawl is of great significance to urban economic development, the detrimental consequences of the urbanization to the urban environment are widespread, especially in most emerging countries.
- The environmental impacts of urbanization are contributed mostly by urban impervious surfaces.

Introduction

- Impervious surfaces are usually defined as the entirety of surfaces through which water cannot pass, including roads, buildings, parking lots, railroads, squares, sidewalks or other urban infrastructure (Arnold and Gibbons, 1996).

- Impervious surface is not only an indicator of the degree of urbanization, but also a major sensitive factor of urban environment.

- In recent years, the impervious surface has become a key environmental indicator in assessing urbanization impacts on the urban environmental, because impervious surface is closely related to many environmental problems, such as water quality, stream health, the urban heat island effect and so on.

- Therefore, impervious surface and its effects on urban environment have attracted more interest recently in the remote sensing community.

Introduction

- Recently, optical imagery has been widely used to estimate the urban impervious surface area, but it has some limitations :

  - The same spectra with different object;
  - The mixed-pixel problem in urban landscapes ;
  - The shadows for high spatial resolution optical images;
  - Impervious surfaces covered by tree crowns.

Introduction

- In order to resolve some of those limitations, our research proposed that RADARSAT-2 full PolSAR data was used for extracting urban impervious surfaces based SVM method.
- The full PolSAR data can provide more useful polarimetric information at spatial and temporal levels for distinguishing different land features.
- The main objective of this investigation is to explore the potential to extract impervious surface area in dense urban areas (e.g., Beijing) from RADARSAT-2 full PolSAR data using SVM method.

Study area and datasets

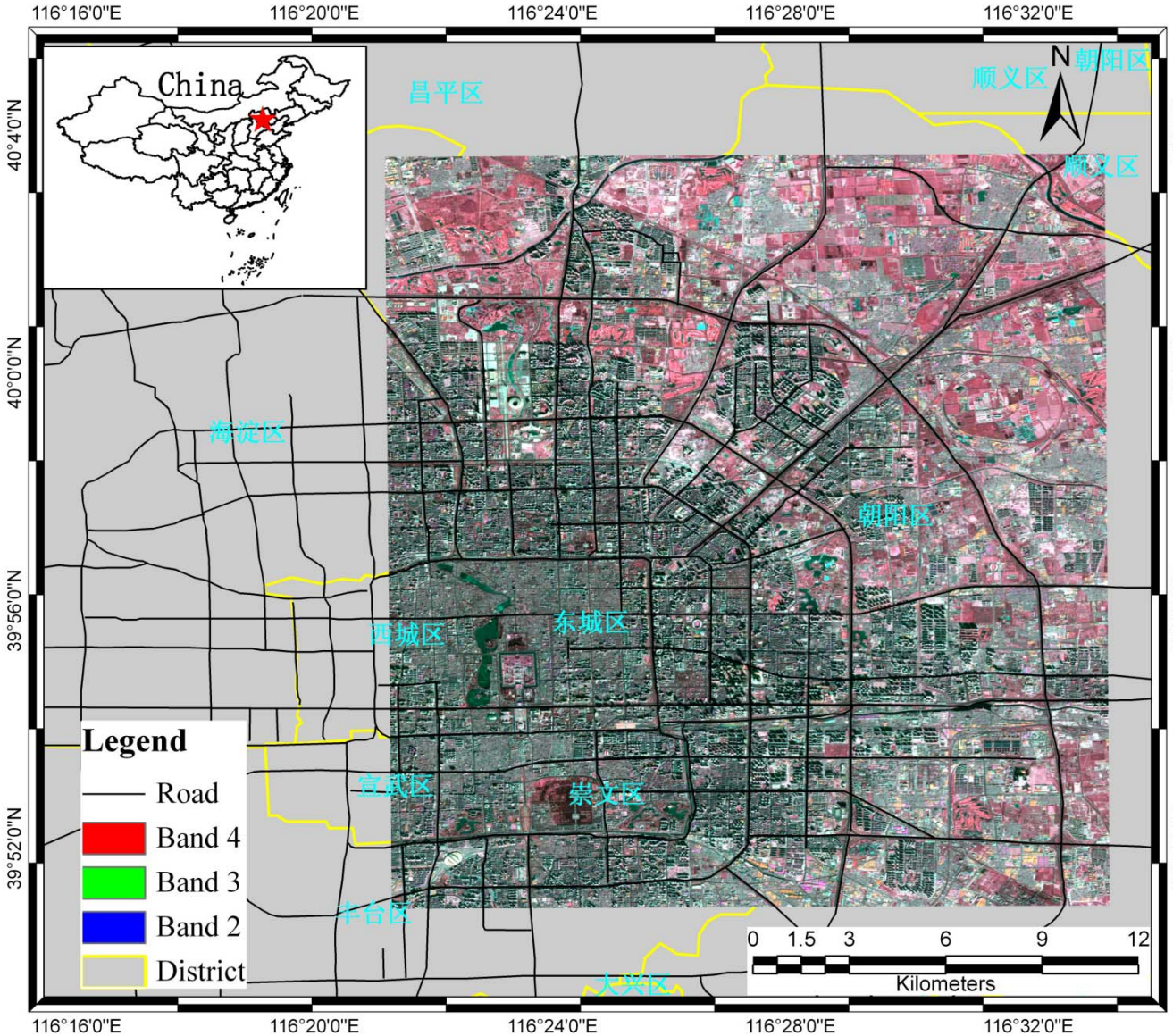

Study area and datasets

Remote sensing datasets used in the research

Datasets	Acquisition date	Spatial resolution	Description
RADARSAT-2	8 Mar. 2009	SLC format with about 12m resolution in slant range and about 8m in azimuth	Full polarimetric data (HH/HV/VH/VV) and C-Band
SPOT-5	12 Jan. 2009	Three VNIR bands with 10m resolution, and one SWIR band with 20m resolution	Cloud free; 2.5m panchromatic band was not used
WorldView	11 Feb. 2009	0.5m resolution	

Study area and datasets

- PolSAR data preprocessing
  - Calibration
  - Multi-look processing(2*1)
  - Speckle filtering(5*5)
  - The pixel size of the neighborhood (5*5)

Methods

SVM model

- SVM implements the Structural Risk Minimization (SRM) principle ;
- SVM converges to a specific solution corresponding to the global minimum of the objective function ;
- In choosing parameters, SVM is less complex than MLPNN. We can easily determine the kernel bandwidth G and the margin C which must be determined in SVM.
- In addition, SVM can obtain better result with less training datasets.

Methods

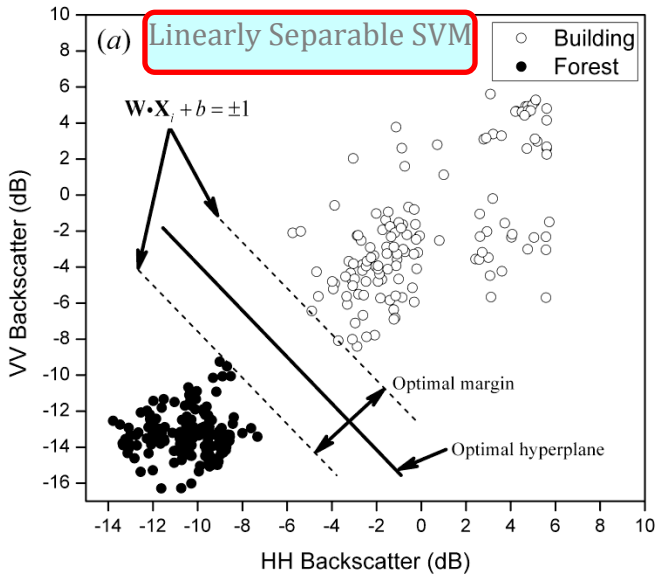

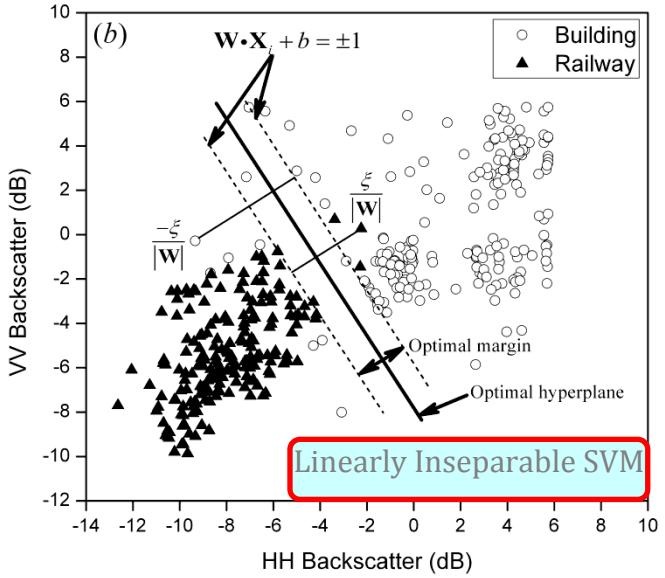

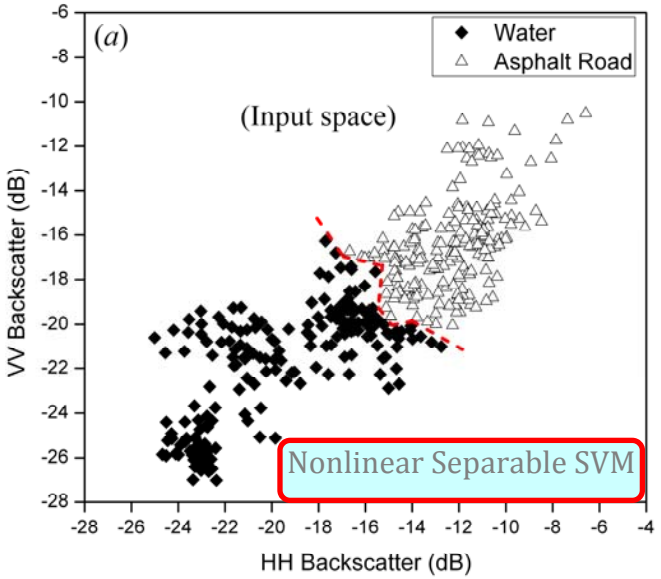

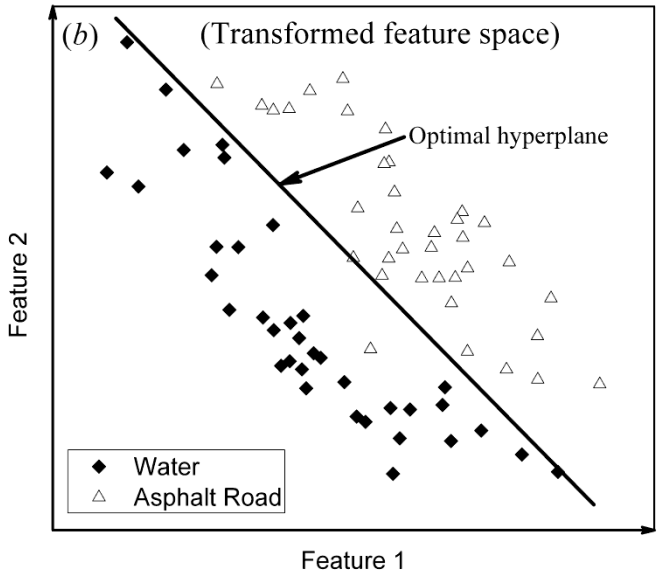

Methods

- SVM model

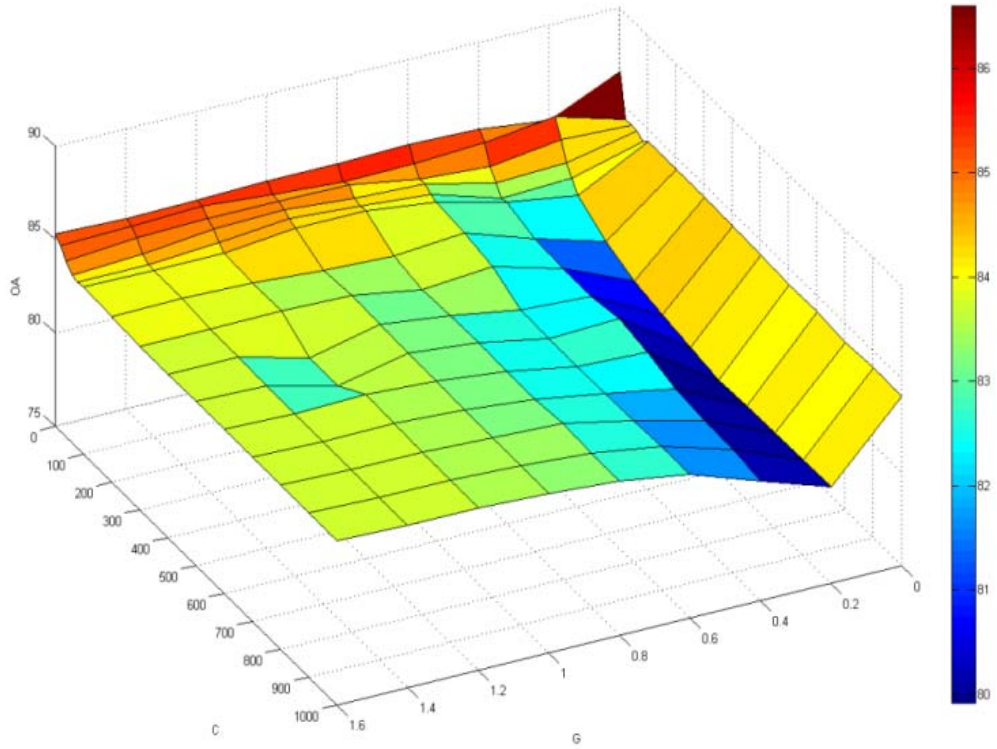

Kernel Function:
Gaussian radial basis function (RBF)
Kernel Width G: 0.5
Penalty Parameter C: 100

Fig. Classification accuracy (OA) using the SVM method with the RBF kernel versus the kernel width G and penalty parameter C.

Methods

- The major land use types in this study
  - Water body
  - Forest
  - Winter crop (wheat)
  - Buildings
  - Bare soil
  - Asphalt road
  - Railway

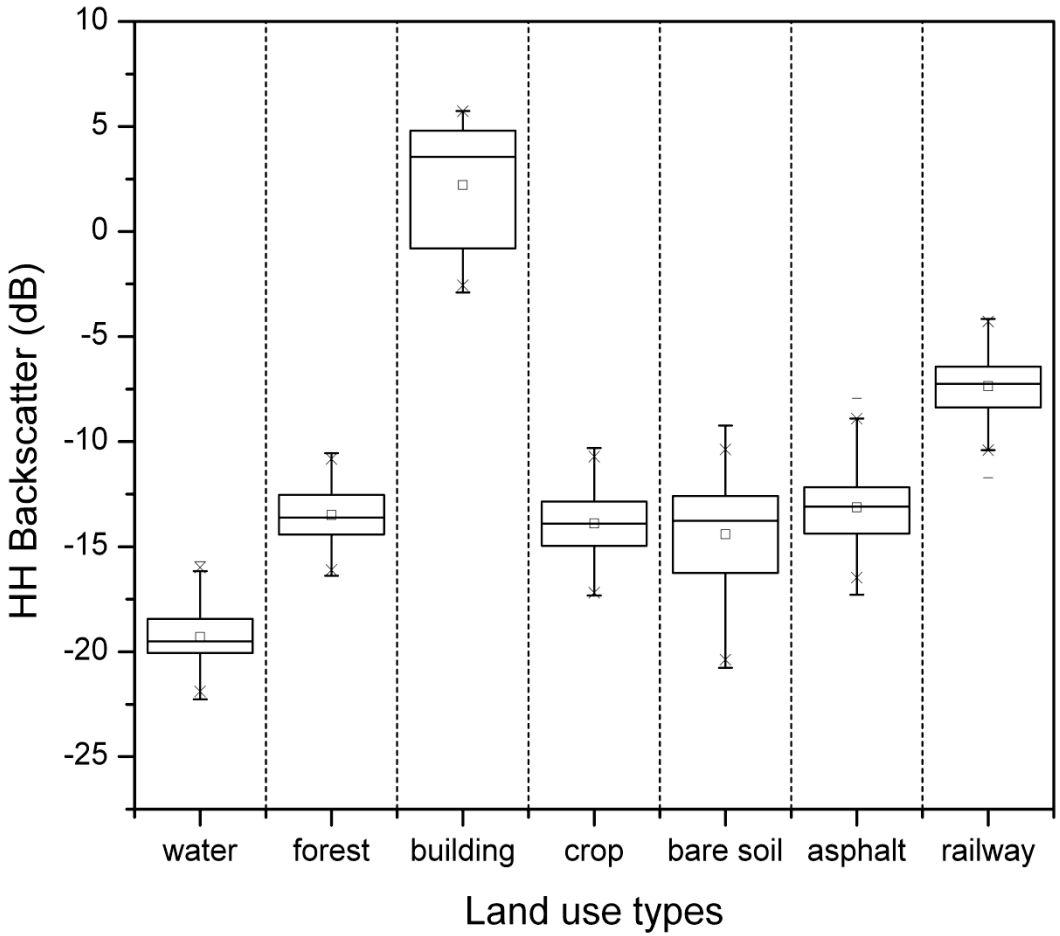

Fig. The variation of backscatter coefficients (HH polarization) for seven land use types at RADARSAT-2 imagery acquisition date in 2009.

Methods

PolSAR features

- The coherency matrix T_3 is defined from a scattering target vector k expressed in the Pauli basis as follows

$$k = \frac{1}{\sqrt{2}} \begin{pmatrix} S_{hh} + S_{vv} \\ S_{hh} - S_{vv} \\ 2S_{hv} \end{pmatrix} \qquad T_3 = \left\langle k \cdot k^{*\mathrm{T}} \right\rangle$$

Polarimetric features assessed for classification

Description	Designation
Elements of the coherency matrix	$T_{ij}(i,j=1,2,3)$
Span	$S = \lvert S_{hh} \rvert^2 + 2\lvert S_{hv} \rvert^2 + \lvert S_{vv} \rvert^2$
Linear intensities ratio	$I_{hv}/I_{hh}, I_{hv}/I_{vv}, I_{hh}/I_{vv}$
Polarimetric coherence between hh and vv polarization	ρ_{hh-vv}
Eigenvalue parameters	$\lambda_1, \lambda_2, \lambda_3, \lambda$
Entropy, anisotropy, α parameters	$H/A/\alpha, \alpha_1, \alpha_2$
Other polarimetric decomposition parameters	Coherent decomposition parameters (Pauli, Krogager) and incoherent decomposition parameters (Huynen, Barnes, Holm, Yamaguchi, Freeman, and Cloude)

PolSAR features datasets

PolSAR coherence | λ | Span

Pauli | Krogager | Freeman

Huynen | Barnes | H/A/α

Cloude | Yamaguchi | Holm

Methods

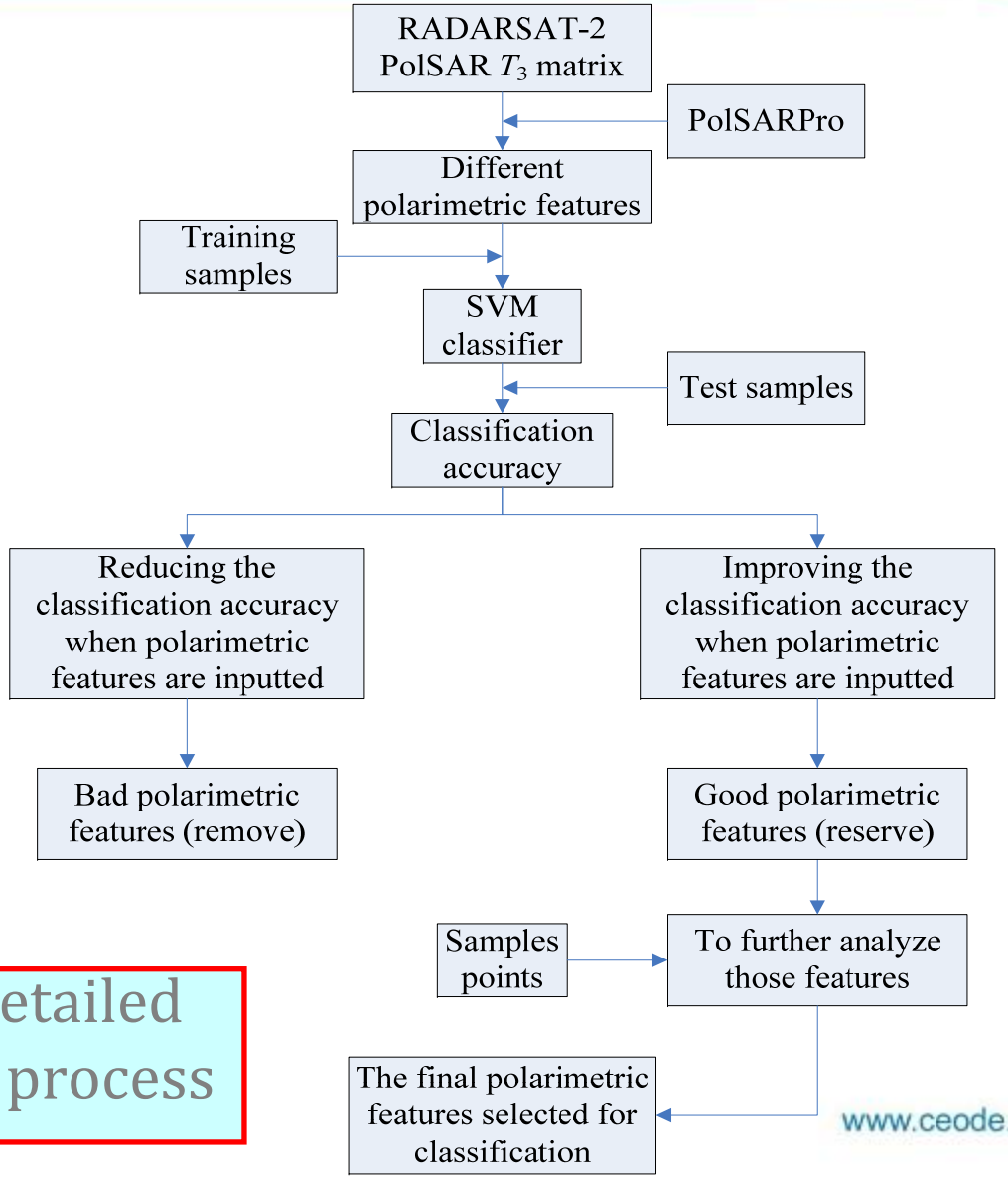

The flow chart of the detailed optimization selection process

Methods

Classification accuracy using different polarimetric features

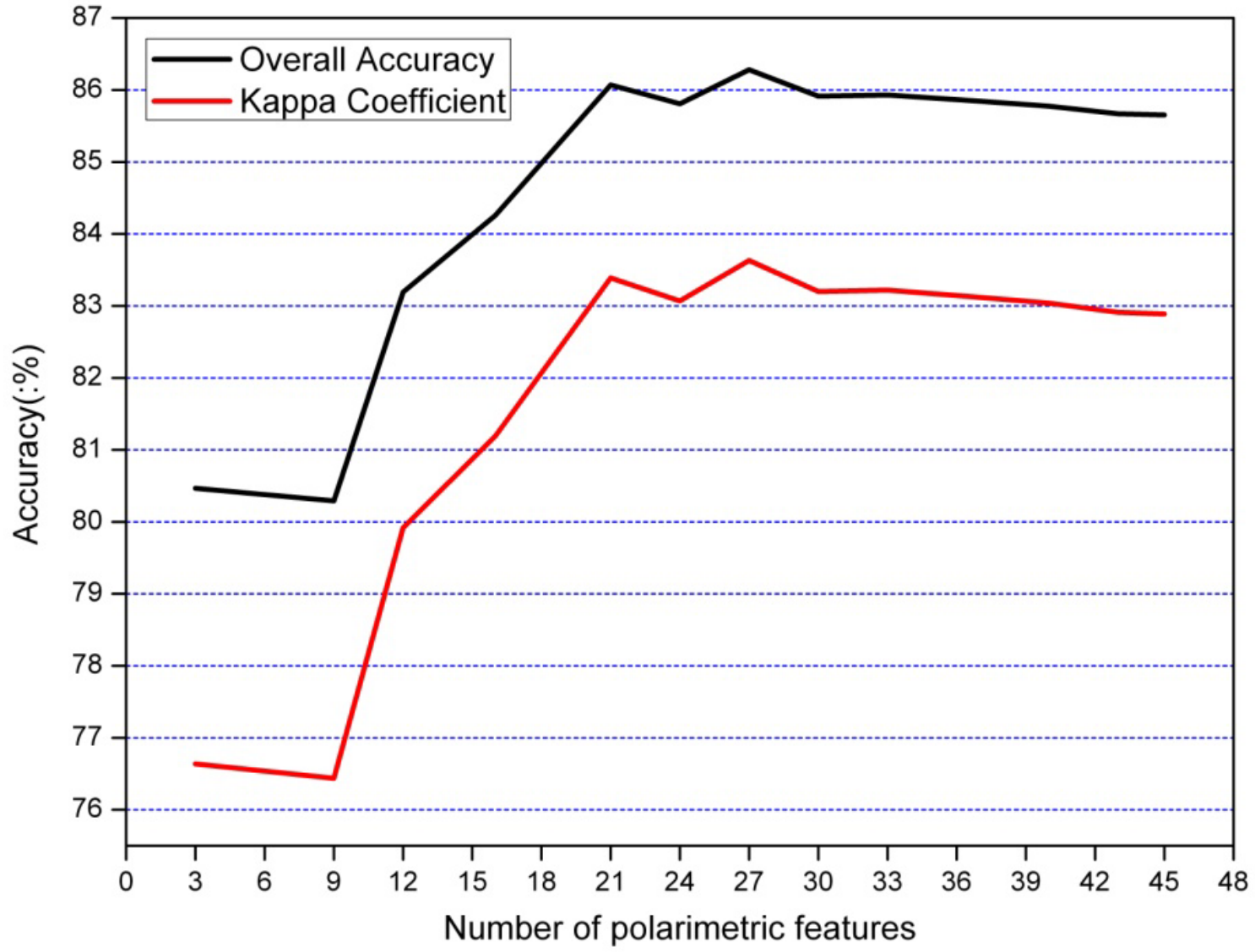

Nu
pol
fea

3
9
10
13
14
18
23
26
29
32
35
39
42
45

ix

nd VV

Methods

The final polarimetric features selected for classification through a stepwise process.

Numbers of polarimetric features	Polarimetric features	Description
3	T_{ii}（i = 1,2,3）	The diagonal elements of T_3 matrix
6	I_{hv}/I_{hh}、I_{hv}/I_{vv}、I_{hh}/I_{vv}	Intensities ratio
8	λ、λ_1	Eigen-value parameters
12	H、A、α、α_1	Entropy, anisotropy, α parameters
14	k_{02}, k_{03}	Barnes decomposition parameters
16	K_S, K_D	Krogager decomposition parameters
20	P_S, P_D, P_V, P_C	Yamaguchi decomposition parameters

Methods

Modeling and mapping impervious surfaces

- According to the definition of impervious surfaces (Arnold and Gibbons, 1996), impervious surfaces in our study area are composed of buildings, asphalt roads, and railway. Thus, the percent of impervious surfaces (PIS) can be calculated by adding buildings, asphalt roads, and railway fraction images (with values ranging from 0 to 1) derived from the RADARSAT-2 full PolSAR image using the SVM method described.

- For the SPOT-5 imagery, four types of training samples were selected, including high albedo, low albedo, vegetation, and soil. By analyzing the relationships between impervious surfaces and the four end-members, Wu and Murray (2003) found that the impervious surface fraction can be calculated by adding low- and high-albedo fractions, while vegetation and soil end-members have little or no contribution to impervious surface estimation.

Methods

Accuracy assessment

- Classification accuracy: Using confusion matrix computed from the validation set, four statistics (overall kappa coefficient (OK), overall accuracy (OA), the producer's accuracy (PA) and the user's accuracy (UA)) were calculated.

- PIS accuracy: A total of 150 sites of 100m×100m were randomly sampled

  - For each sample, the impervious surface was digitized on the corresponding high-quality WorldView images with a spatial resolution of 0.5m. Then, PIS was calculated for each site.

  - 3 statistical indicators between estimated PIS and the reference data (root mean square error (RMSE), mean absolute error (MAE), and the coefficient of determination (R^2)) and their scatter plots were used to evaluate the accuracy of the PIS estimation.

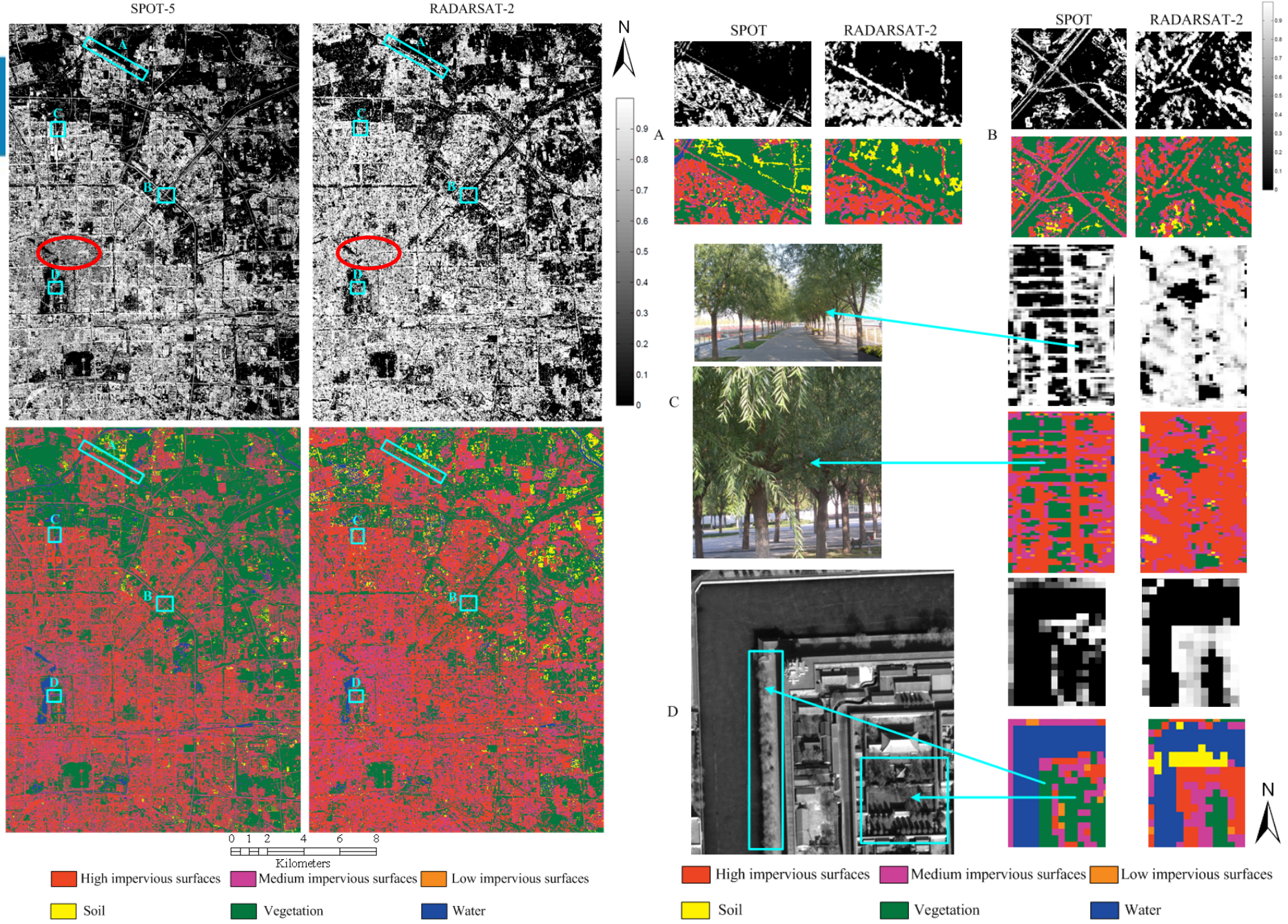

Extracted impervious surfaces

Impervious surface of four sample sites

Results and analysis

1. There is more bare soil in the PIS classification image derived from RADARSAT-2 data than that from SPOT-5 image. RADARSAT-2 PolSAR (C-Band) has deeper penetration. On 8 March 2009, the main crop of the study area was small and short winter wheat. C-Band can penetrate winter wheat and detect bare soil.
2. In selected sample area A, because of stronger backscattering in SAR images, the railroads can be easily extracted from RADARSAT-2 full PolSAR data; while SPOT-5 imagery cannot extract them.
3. Because of intrinsic characteristics of SAR imagery(such as layover and shadow effects) , the entire road area might be either occluded by shadows or covered by layover from adjacent buildings or trees, which become a severe problem for extracting impervious surfaces, especially in dense urban areas.
4. Compared with optical imagery, PolSAR imagery has enormous potential for extracting the impervious surfaces covered by tree crowns in wooded areas, especially in area with sparse cover.

Results and analysis

Confusion matrix and classification accuracy of the SVM classifier.

Confusion matrix of SVM classifier										
Reference data										
	Type	Water	Forest	Building	Crop	Soil	Asphalt Roads	Railroads	Total	UA (%)
Classified data	Water	**1086**	0	0	0	8	0	0	1094	99.27
	Forest	0	**806**	0	62	0	32	23	923	87.32
	Building	0	0	**909**	0	0	0	69	978	92.94
	Crop	0	286	0	**690**	3	28	3	1010	68.32
	Soil	0	1	0	74	**288**	26	0	389	74.04
	Asphalt Road	0	29	0	0	6	**934**	0	1030	90.68
	Railroads	0	35	5	0	7	0	**265**	305	86.89
	Total	1086	1157	914	826	366	1020	360	**5729**	
	PA (%)	100.00	69.66	99.45	83.54	78.69	91.57	73.61		
	OK	**0.8437**								
	OA (%)	**86.89**								

Note: UA = user's accuracy; PA = producer's accuracy; OK = overall Kappa; OA= overall accuracy.

Results and analysis

1. SVM can provide significantly better classification performance. OA and OK are 86.89% and 0.8437.

2. For the building class, the PA and UA are 99.45% and 92.94% with the SVM. The water class had higher PA (100.00%) and UA (99.27%).

3. Water and building could be easily separated from other land use types, and soil and water could be absolutely distinguished from the buildings and asphalt roads using full PolSAR data.

4. Because there is some vegetation on the sides of roads, creating mixed-pixel problem, the asphalt roads or railroads tend to be misclassified as vegetation.

Results and analysis

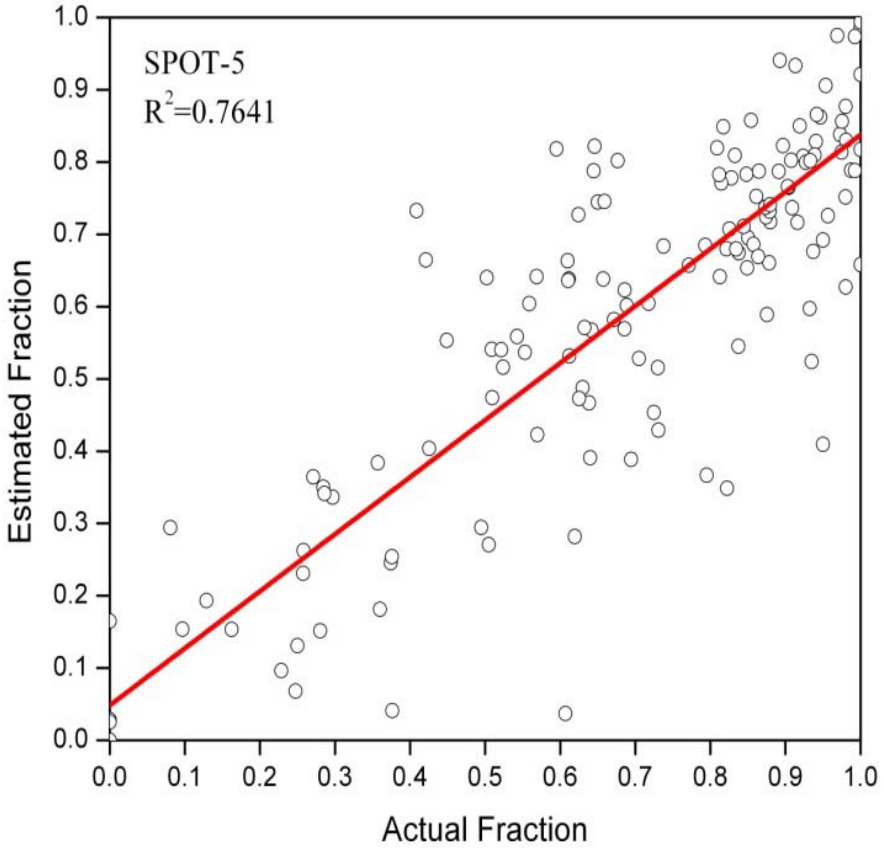

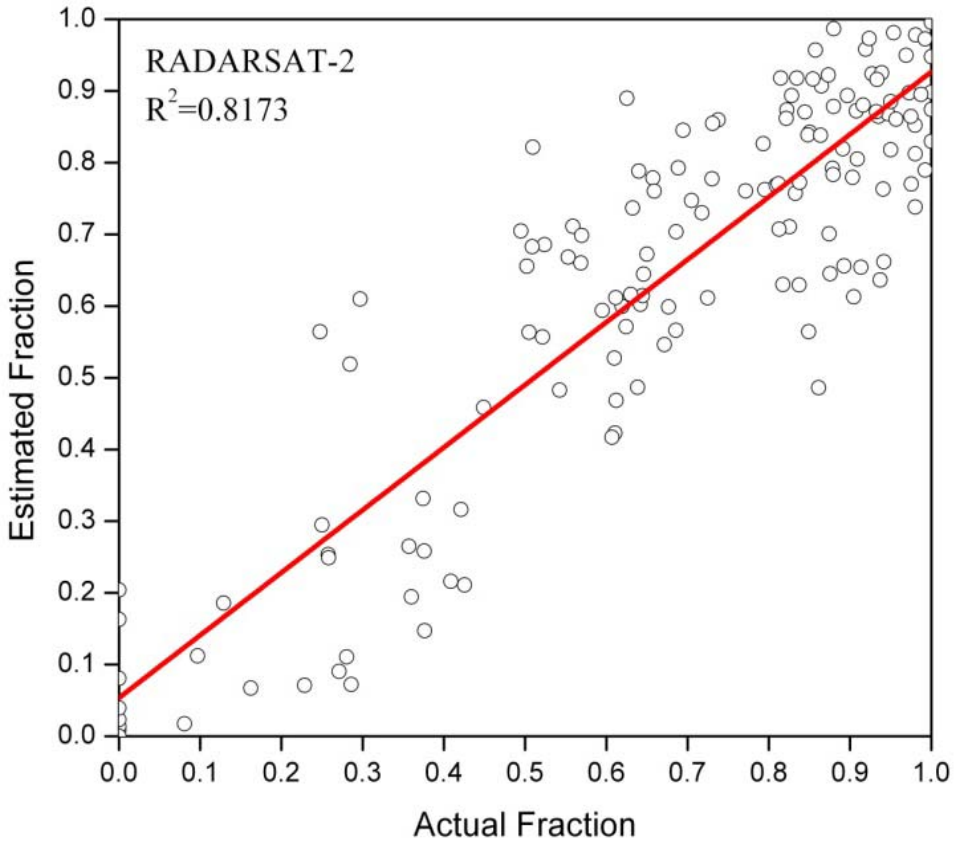

Scatter plots of the accuracy assessment of impervious surface estimation

Conclusions

- It shows that RADARSAT-2 data can provide more accurate estimations than that of SPOT-5;
- PolSAR imagery has enormous potential for extracting the impervious surfaces covered by tree crowns in wooded areas, especially in sparsely wooded areas.
- The mixed-pixel problem is a major problem for both data, affecting the accuracy of impervious surface estimation.
- Some intrinsic characteristics of SAR imagery become a severe problem for extracting impervious surfaces, especially in dense urban areas.
- Overall, our results demonstrate that PolSAR imagery can provide more efficient and useful polarimetric information and has enormous potential for extracting impervious surfaces.

Conclusions

Future work

- More effective optimization selection method for polarimetric parameters
- Modified SVM which suitable for SAR datasets

Thanks



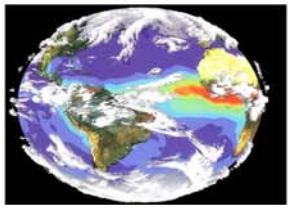
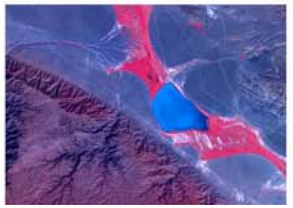

Center for Earth Observation and Digital Earth

Chinese Academy of Sciences

Add:No.9 Beiyitiao Road, Zhongguancun, Beijing China 100190

Tel:86-10-58887301 Fax:86-10-58887302

E-mail:office@ceode.ac.cn

Web:www.ceode.ac.cn